

## Water Purification from Organic Pollutants using a Photo-Oxidation

<sup>1</sup>Bhishma Karki, <sup>1</sup>Jeevan Jyoti Nakarmi and <sup>2</sup>Mukesh Jerambhai Keshavani

<sup>1</sup>Central Department of Physics, Tribhuvan University, Kirtipur, Kathmandu, Nepal

<sup>1,2</sup>Department of Physics, Marwadi University, Rajkot, 360003 Gujarat, India

**Abstract:** Water treatment scheme is proposed where two variables are taken. BiVO<sub>4</sub> photoanode combined with a thin film silicon solar cell. It has a band gap energy of 2.4 eV which has good catalytic properties for the degradation of phenol and chloroform. Applying an external bias voltage in order to reach the required potentials for pollutant degradation. To cover the voltage needs, an a-Si:H/nc-Si:H solar cell was coupled with the BiVO<sub>4</sub>. This solar cell was specifically designed to work under the transmitted spectrum of the BiVO<sub>4</sub> with thicknesses of 200 and 1000 nm for the top and bottom cell, respectively. This device has successfully been fabricated and tested for removal of organic contaminants from an aqueous solution. The device with the solar cell performed better than, the BiVO<sub>4</sub> photoanode alone with a similar external bias voltage applied, suggesting that the solar cell does not only act as a voltage source but also as a current source. To compare the performance of this device to the commercially available ZnO photoanode illuminated by UV light, an energy balance for phenol removal was performed. The energy needed for phenol removal was reduced from 1.83 Wh/mg with the ZnO/UV device to 0.79 Wh/mg with the BiVO<sub>4</sub> with a solar cell indicating the potential of the proposed device to improve the water treatment of organic pollutants by using Earth-abundant materials and solar energy.

**Key words:** Solar energy, photo-oxidation, organic pollutants indicating, improve, water treatment, silicon

### INTRODUCTION

The most pressing environmental problems associated with the growing world population are the lack of clean water insufficient food production and a sustainable generation and consumption of energy. Currently, billion people have no access to electricity (World Bank) and a similar number of people have no access to clean water. These problems cannot be tackled independently from each other, since, poor electrification goes together with the lack of access to clean water. Hazardous effluents pollute many major water supplies, caused by heavy industrialization and urbanization. Among the most common contaminants are organic pollutants such as pesticides, pharmaceuticals, phenol compounds, chloroform or dyes (Alahmadi *et al.*, 2018; Martinez-Huitle and Brillas, 2009). Currently, these pollutants are hardly removed using traditional methods like filtration, chemical coagulation or aerobic and anaerobic treatment (Martinez-Huitle and Brillas, 2009; Bennani *et al.*, 2015). In this research, we decouple these competitive metrics by proposing a solar-powered photoelectrochemical solution. Low final concentrations of pollutants are expected to be obtained by using photoelectrochemical methods and low cost-prices are obtained using free solar energy in combination with cheap, abundant materials (Anonymous, 2013, 2019).

In particular, photoelectrochemical oxidation is able to remove toxic organics, ecologically hazardous cyanides and other residual compounds even at low concentrations being, therefore, an ideal candidate for advanced water purification (Sarkka *et al.*, 2015). This method uses the light absorbed in a semiconductor to degrade the pollutants into less complex compounds that can be easier to remove by a post-treatment step. By either using a photoanode or a photocathode, oxidation or reduction of pollutants is possible, allowing different pollutants to be treated. In the research, the focus is on the photo-oxidation of organic pollutants using an n-type photoanode (Chong *et al.*, 2010; Cotal *et al.*, 2009).

Among the candidates for photo-oxidation, metal oxides have been the most extensively used materials with bismuth-based compounds (Dette *et al.*, 2014; Al-Hamdi *et al.*, 2016) SnO<sub>2</sub>, WO<sub>3</sub> and TiO<sub>2</sub> as examples. In particular, TiO<sub>2</sub> has been widely used as the semiconductor of choice for photo-oxidation of pollutants, since, it is cheap and chemically stable. However, its bandgap energy is rather high (3.2 eV), meaning that it can only be excited by UV light. Therefore, this material is very energy intensive, making the process less cost-effective.

In this research, BiVO<sub>4</sub> was used as a photoanode due to its bandgap energy of ~2.4eV, high stability and low price. BiVO<sub>4</sub> is already used as a yellow pigment for paint and has been successfully demonstrated as a promising

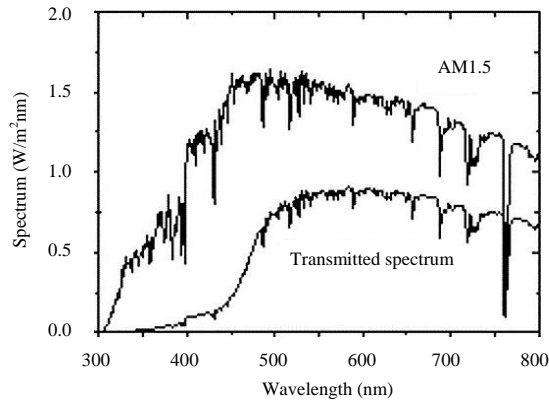


Fig. 1: Spectrum compared to the transmitted spectrum after the  $\text{BiVO}_4$  photoanode

photoanode for solar water splitting. However, a potential is needed inside the material, so that, the charge carriers are able to deliver enough energy to drive the reaction. Since, these semiconductors are not able to produce these potentials by themselves, an external bias voltage is needed. Here, we propose to use a solar cell that utilizes the spectrum transmitted by the  $\text{BiVO}_4$  photoanode (Fig. 1) to create the voltage needed as extra bias. The options available include III-V technologies, perovskites, crystalline Silicon (c-Si), thin-film amorphous and nanocrystalline Silicon (a-nc-Si) and CIGS (Daskalaki *et al.*, 2013). In order to choose the most suitable technology, it must be noted that the optimum external bias voltage is 1V. Therefore, multijunction solar cells which consist of several cells monolithically stacked and series connected, may be required. Thin-film silicon was used due to the flexibility of its design, know-how on possible multijunction devices and stability of the devices and the low cost of materials. A thin-film silicon solar cell was specially designed to work in this device and was successfully integrated, demonstrating the viability of this device (Al-Hamdi *et al.*, 2016).

To tackle all challenges mentioned above, this study proposes a new photoelectrochemical water purification system that operates spontaneously using only solar irradiation and no external power supply. It consists of a photoanode combined with a solar cell and a conductive cathode counter electrode. This device has the potential to reduce the costs by using free solar energy and Earth-abundant materials, to achieve low final pollutant concentrations by using advanced photo-oxidation methods and to have the additional advantage of being electrically autonomous from any external power source.

Combining all these elements, a bias-free demonstrator based on Earth-abundant materials for organic pollutant removal was realized. This is the first

time that a multijunction approach is used for better spectral utilization in a pollutant removal photo-oxidation process.

## MATERIALS AND METHODS

**Experimental details:**  $\text{BiVO}_4$  fabrication. Asahi UV type textured glass was cleaned with a sequence of acetone and isopropanol and used as a substrate for  $\text{BiVO}_4$  thin film deposition. Prior to the  $\text{BiVO}_4$ , a 5 nm  $\text{SnO}_2$  layer was deposited by spray pyrolysis at  $480^\circ\text{C}$  to avoid recombination in the interface with the Transparent Conductive Oxide (TCO). The precursor for  $\text{BiVO}_4$  spraying was made by mixing equimolar quantities of  $\text{Bi}(\text{NO}_3)_3 \cdot 5\text{H}_2\text{O}$  (98% Alfa Aesar) solution in acetic acid (98% Sigma Aldrich) with  $\text{V}(\text{AcAc})_2$  (99% Alfa Aesar) solution in absolute ethanol (Sigma Aldrich). This precursor solution was then deposited by spray pyrolysis at  $450^\circ\text{C}$  at a rate of 0.2 mL/sec. Cycles consisting of 5 sec of spraying plus 55 sec of idle to evaporate the solvents were performed. An annealing step at  $450^\circ\text{C}$  for 2 h followed in order to achieve the desired crystal structure. The  $\text{BiVO}_4$  thin films had a thickness of 200 nm. The contacts consisted of a 200 nm Al stripe on the TCO deposited by Electron Beam Physical Vapor Deposition (EBPVD). For the experiments involving only the  $\text{BiVO}_4$ , an active area of  $16 \text{ cm}^2$  was used while for the combination of the solar cell, this was reduced to  $1 \text{ cm}^2$  due to limitations in the TCO conductivity of the solar cell.

**Solar cell fabrication:** The solar cells were deposited by Plasma Enhanced Chemical Vapour Deposition (RF-PECVD) using a cluster tool from Electrorava. The a-Si:H and a-Si:H/a-Si:H solar cells were deposited on Asahi UV substrates while the a-Si:H/nc-Si:H solar cells were deposited in wet etched textured glass with Aluminium-doped Zinc Oxide (AZO) as a TCO. The texturing of the glass is described elsewhere.

Nanocrystalline Silicon Oxide (nc-SiOx) has been used as P-layer (boron doped) and n-layer (phosphorous doped). The thickness of the absorber layers (intrinsic a-Si:H and nc-Si:H) has been varied by varying the deposition time. The deposition rates of a-Si:H and nc-Si:H were 0.16 and 0.71 nm/sec, respectively. The contacts have been deposited using Electron Beam Physical Vapour Deposition (EBPVD). A 200 nm aluminum stripe in contact with the TCO has been used as front contact. A stack of 150 nm silver, 20 nm chromium and 400 nm aluminum has been used as back reflector and back contact. The solar cell area was  $1 \text{ cm}^2$ .

**Solar cell characterization:** External Quantum Efficiency (EQE) was measured to obtain the amount of charge carriers generated per photon of a given

wavelength incident on the solar cell. The JV curves of the solar cells have been measured using a two Xe lamp flash PASAN solar simulator (Class AAA) and corrected by the short-circuit current obtained from the integration of the EQE measurements. The BiVO<sub>4</sub> photoanode has been used as a filter to obtain the transmitted spectrum during both measurement.

#### Photoelectrochemical measurements and sampling:

Photoelectrochemical experiments for phenol and chloroform degradation were carried out with a set-up consisting of a cylindrical quartz glass reactor with an effective vessel volume of 300 mL, an Atlas solar simulator (SUNTEST XXL+) and a three-electrode configuration with an Ag/AgCl reference electrode. The initial volume of the working solution was 250 mL phenol ( $\geq 99\%$ , Sigma Aldrich) with initial concentration of 20 and 250 mL chloroform solution (Baker analyzed, containing 0.75% ethanol as stabilizer) with initial concentration of 500 ppb. Demineralized water (RiOs 5 Reverse Osmosis system) was used throughout the experiments for dilution. To eliminate the influence of solution resistance, 0.1 M Na<sub>2</sub>SO<sub>4</sub> was chosen as supporting electrolyte. The 2 mL samples of phenol solution and 25 mL of chloroform solution were collected from the reaction solution at regular time intervals (every 1 h). The 2 mL of phenol solution sample were added to a cuvette and measured with UV/Vis spectrophotometer (Hach Lange DR 5000, cuvette tests LCK 345 with a measuring range of 0.05-5.00, 5-50 and 20-200 mg/L) to determine the residual concentration of phenol. Phenol reacts with 4-nitroaniline to form a yellow-colored complex which is then measured by photometry. The possible measurement error of the spectrophotometer is  $\pm 5\%$ .

At the start of each experiment, the BiVO<sub>4</sub> electrodes were kept in the stirred phenol and chloroform solution in the dark for 1 h for adsorption to reach equilibrium. In order to get an insight into the effect of the counter electrode on the PEC performance of the above-described system, three counter electrodes were used. A graphite plate was used as a cathode in the experiments. To investigate the effect of the cathode on the PEC performance, carbon foam and a copper plate were additionally tested.

The pH of the solution was kept constant at 7.2 and was measured before the experiment, using a Sentix 81 pH meter. The temperature was controlled at  $25 \pm 1^\circ\text{C}$  by recirculating cooling water in a water bath equipped with cooler Julabo, FL300. During the experiments, the reactor was closed by a UV permeable quartz lid to prevent evaporation of phenol. The electrode potential and working current were controlled with a potentiostat-galvanostat system.

The phenol and chloroform photodegradation experiments using only the BiVO<sub>4</sub> photoanode were

performed by applying the optimal potential of 1 V (vs. Ag/AgCl, KCl saturated) which was taken from previous studies.

In the case of the combination with the solar cell, a Voltage of 0 V (vs. Ag/AgCl KCl saturated) was applied. The net current was determined by subtracting the dark current from the photocurrent.

## RESULTS AND DISCUSSION

In order to understand and improve the PEC performance of the proposed system, each of the active components (BiVO<sub>4</sub>) photoanode, counter electrode and supporting solar cell) were studied separately. In addition, an energy balance of the newly proposed bias-free system was performed and compared with the more traditional systems based on a ZnO photoelectrode.

BiVO<sub>4</sub> photoanode. BiVO<sub>4</sub> has been previously successfully demonstrated as a photoanode for treatment of organic pollutants. However, when integrated in a working device, other variables such as scalability or stability are important. In addition, it is preferable that this device can treat different contaminants. Here, these features are considered to assess the suitability of BiVO<sub>4</sub> for this device.

Regarding the stability of the BiVO<sub>4</sub> photoanode, four consecutive degradation cycles were performed on the same sample. The results in Fig. 1 show the constant rates of degradation (k), obtained and normalized by dividing by the average k value (black line). The reaction rate constant remained within  $<10\%$  of the initial value for the 4 consecutive cycles tested. The possible measurement error of the spectrophotometer is  $\pm 5\%$  and the maximum error of the fitting was  $\pm 2.5\%$ . Therefore, the added possible error of these measurements is 7.5%, represented in Fig. 2 by the dashed lines. That shows that the variations observed in the reaction rate constant among the different measurements can be due to measurement inaccuracies and the photoelectrode can be considered stable.

Finally, the flexibility of pollutants that can be treated with BiVO<sub>4</sub> must be taken into consideration for a practical water treatment device. BiVO<sub>4</sub> is a promising material for water treatment of organic pollutants, not only for phenol degradation but also for other organic compounds such as dyes. To further assess the flexibility of BiVO<sub>4</sub> regarding pollutants, the degradation characteristics of phenol and chloroform were measured and the results are shown in Fig. 3a. The reaction rate constants according to first order kinetics can be determined to be 0.0053 and 0.0075 min<sup>-1</sup> for phenol and chloroform, respectively.

This shows that BiVO<sub>4</sub> performed even better for chloroform removal than for phenol removal with a higher reaction rate constant and reaching a final concentration of 17% of the initial in 4 h. To determine, if this effect

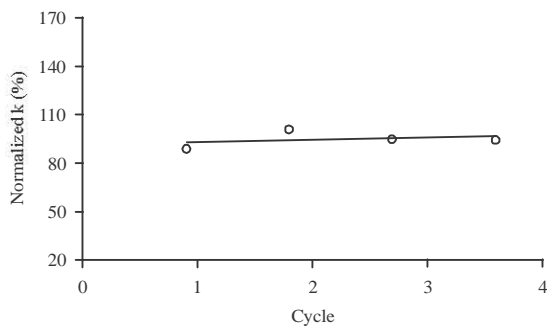


Fig. 2: Reaction rate constant  $k$  normalized by the average reaction rate constant for several consecutive cycles on a  $\text{BiVO}_4$  photoanode with applied bias voltage of 1 V (vs. Ag/AgCl, KCl saturated). The percentage represents how much the reaction rate constant has change with respect to the average value (black line). The dotted lines represent the estimated possible error inherent to the measurement equipment and fitting procedures (7.5%)

might be due to the different light absorption of the two pollutants, this absorption was measured as shown in Fig. 3b. The absorption peak for phenol is at 200 nm and the absorption peak for chloroform is found at 215 nm. Since, the solar spectrum used for these experiments, showed in yellow in Fig. 3b, contains low amounts of light at wavelengths lower than 300 nm, none of the solutions will absorb a significant part of the solar spectrum and thus, the light absorption in the solution can be ruled out as a negligible factor. Therefore, the differences in degradation of pollutants observed in Fig. 3a would mainly be caused due to enhanced adsorption and reaction rates on the photoanode surface for chloroform removal. In particular, some literature reports that  $\cdot\text{OH}$  radical addition can more easily target C-Cl bonds rather than C-H bonds. Phenol was the used contaminant for further investigation as the “worst case” scenario in this study.

Counter electrode the cathode material is where the hydrogen evolution reaction occurs, completing the circuit and redox reaction. It can affect the overall degradation reaction by electro-reduction of the dissolved oxygen into  $\text{H}_2\text{O}_2$ , electro-reduction of the organic pollutants or direct adsorption of these contaminants in porous cathodes (Demeestere *et al.*, 2007).

In order to study the interaction between the electrochemical oxidation and reduction reactions and to minimize the over-potential related to the counter electrode, different materials and configurations were tested. Ag, Al, Au, Cu, Ni, Pb, Pd, Pt, Ti, Zn, graphite, glassy carbon and Activated Carbon Fiber (ACF) have been proposed in literature as cathode materials in the electrochemical treatment of water containing different

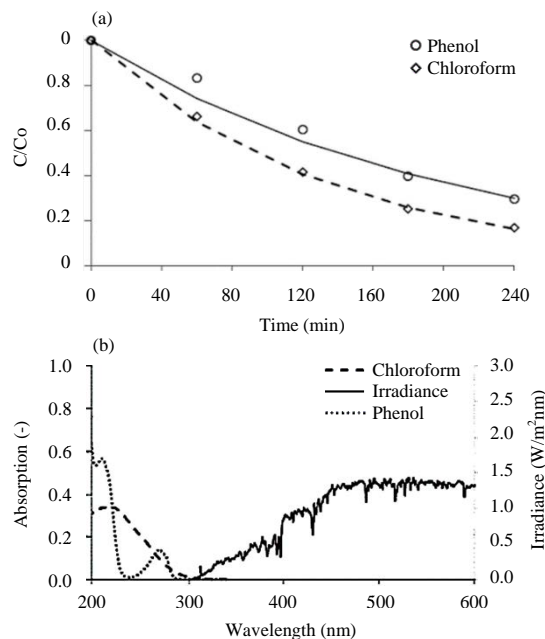


Fig. 3: a) Degradation of phenol and chloroform solutions using a  $\text{BiVO}_4$  photoanode with an applied bias voltage of 1 V (vs. Ag/AgCl, KCl saturated) and corresponding fitting considering first order kinetics and b) Light absorption of the phenol and chloroform solutions used, compared to the solar irradiance (right axis)

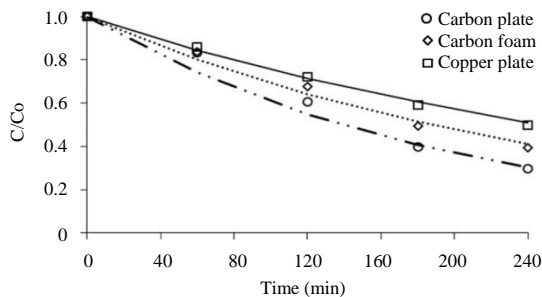


Fig. 4: Phenol degradation related to the used counter electrode and corresponding fitting considering first order kinetics

organics pollutants (Fan *et al.*, 2006). In this study, Cu and graphite were studied due to their relative low cost with respect to other more precious metals and high removal efficiency. The results are presented in Fig. 4.

The reaction rate constants obtained by fitting to a first order reaction are  $0.0053 \text{ min}^{-1}$  for the carbon plate counter electrode,  $0.0040 \text{ min}^{-1}$  for the carbon foam and  $0.0029 \text{ min}^{-1}$  for the copper plate. Therefore, carbon seems to be the best material to use as counter electrode. This might be due to the generation of  $\text{H}_2\text{O}_2$  on carbon



electrodes which helps the reaction by adding the possibility of homogeneous catalysis. In addition, copper electrodes have a tendency to reduce the dissolved oxygen present in the aqueous phenol solution, negatively influencing phenol degradation. Dissolved oxygen acts as an effective electron acceptor to extend the hole's lifetime and to form the oxidizing species of hydroxyl radicals, affecting the photoactivity of the BiVO<sub>4</sub> film. Finally, despite the fact that carbon foam has a higher surface area, the carbon plate performs better, probably due to the easier mass transport to the surface.

Solar cell BiVO<sub>4</sub> needs a potential applied in order to work at its optimum, since, the electrochemical potential of the reaction is higher than the one produced by the BiVO<sub>4</sub> photoanode by itself. In previous studies, it was determined that the optimum external applied bias for phenol degradation was 1V vs. Ag/AgCl (Han *et al.*, 2014; Huang *et al.*, 2015). In order to apply the needed potential, an additional solar cell can be added to the system. In this study, thin-film silicon solar cells were used in combination with the BiVO<sub>4</sub> photoanode due to its flexibility of design regarding the output voltage and current. Using this material, a multijunction approach can be used allowing for higher operating voltages than single junctions and better spectral utilization. Using this approach, it is possible to have the Si solar cells produce the applied potential of 1 V at operational conditions, making the system autonomous and removed from an external power supply.

Three main options were explored to use as solar cell: a-Si: H single junction, a-Si: H/a-Si: H double junction and a-Si: H/nc-Si: H double junction. Since, the spectrum reaching the solar cells is not AM1.5 but the spectrum transmitted by the BiVO<sub>4</sub> Fig. 1, the absorber thicknesses were adjusted to optimize the output parameters, setting a boundary condition that the a-Si:H top absorber layers would not increase further than 200 nm to avoid strong light-induced degradation. For the a-Si: H/a-Si: H solar cell, the used top and bottom absorber thickness were 150 and 400 nm, respectively. The open-circuit voltage achieved with these cells was 1.59 V and the short-circuit current under the transmitted spectrum was 2.27 mA/cm<sup>2</sup>. Regarding the a-Si: H/nc-Si: H cell, the bottom cell absorber thickness was fixed at 1000 nm and the top cell absorber thickness was optimized at 200 nm.

The short circuit current under the transmitted spectrum in that case was 3.86 mA/cm<sup>2</sup> and the open circuit voltage was 1.27 V. Finally, the single junction a-Si: H cell of 200 nm was chosen which had a short circuit current under transmitted spectrum of 4.85 mA/cm<sup>2</sup> and an open circuit voltage of 0.83V. Figure 5a shows the different JV characteristics of the solar cells with optimum thicknesses and Fig. 5b shows the EQE measurements. It can be noticed from the EQE measurements that, even there is still room for improvement, there is good current matching of the tandem junction cells.

Table 1: Energy balance results for different configurations

Materials	Light (W/m <sup>2</sup> )	Bias Voltage (V)	E (Wh/mg)
ZnO	UV (125)	0	1.83
ZnO	AM1.5 (1000)	1	4.21
BiVO <sub>4</sub>	AM1.5 (1000)	1	1.15
BiVO <sub>4</sub>	AM1.5 (1000)	Solar cell (0V)	0.79

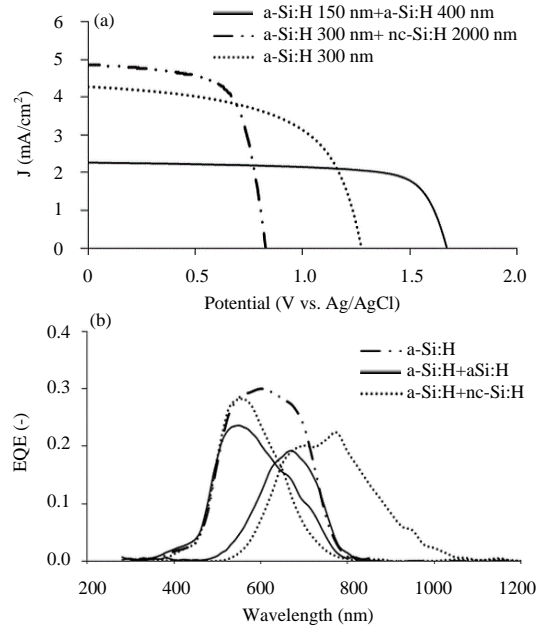


Fig. 5: (a) JV characteristics and (b) EQE measured with the BiVO<sub>4</sub> transmitted spectrum of the a-Si: H/a-Si: H tandem solar cell (-); a-Si: H/nc-Si: H (....) solar cell and a-Si: H single junction cell (-.-.). The corresponding short-circuit currents extracted from the EQE are shown in the graph in the corresponding color

The BiVO<sub>4</sub> photoanode was combined with the optimized solar cells of each technology presented, obtaining the phenol degradation curves displayed in Fig. 5.

The conditions of each analyzed system, together with the energy needed per mg removed are displayed in Table 1. The systems compared are the BiVO<sub>4</sub> photoanode with and without the solar cell, a ZnO/Zn composite illuminated by the solar spectrum and a ZnO based photoanode illuminated by UV light.

The differences between the UV/ZnO system (Tyagi *et al.*, 2013) and the ZnO/Zn plate system is mainly due to the different energies of the light sources, stressing the fact that if UV light is used, the ZnO photoelectrode performance is better than with AM1.5.

The BiVO<sub>4</sub> photoanode performed better than ZnO in all cases, due to the improved phenol degradation characteristic. The use of BiVO<sub>4</sub> alone instead of ZnO

with AM1.5 reduced the energy input needed per mg treated by more than 70%. When the solar cell was introduced, the situation was further improved by reducing the energy needed to 0.79 Wh/mg of degraded phenol. It is important to note that most of the input energy in the AM1.5 cases would be coming directly from the sun and not from an external source of energy like it would be in the case for the ZnO with UV light.

### CONCLUSION

The reduction of the energy needed with the designed device would translate in a smaller, more compact equipment in a practical device, potentially reducing the costs of materials and installation. That makes the system more cost-effective. In addition, an autonomous system from external power sources would allow installation not only in main urban areas but also in remote rural places with no access to electricity.

### REFERENCES

- Al-Hamdi, A.M., M. Sillanpaa, T. Bora and J. Dutta, 2016. Efficient photocatalytic degradation of phenol in aqueous solution by SnO<sub>2</sub>:Sb nanoparticles. *Appl. Surf. Sci.*, 370: 229-236.
- Alahmadi, N.S., J.W. Betts, T. Heinze, S.M. Kelly and A. Koschella *et al.*, 2018. Synthesis and antimicrobial effects of highly dispersed, cellulose-stabilized silver/cellulose nanocomposites. *RSC Adv.*, 8: 3646-3656.
- Anonymous, 2013. Improved water source (% of population with access). The World Bank, Washington, DC., USA. <https://datacatalog.worldbank.org/improved-water-source-population-access>
- Anonymous, 2019. Access to electricity (% of population). The World Bank, Washington, DC., USA. <https://data.worldbank.org/indicator/EG.ELC.ACCS.ZS>
- Bennani, Y., P. Appel and L.C. Rietveld, 2015. Optimisation of parameters in a solar light-induced photoelectrocatalytic process with a TiO<sub>2</sub>/Ti composite electrode prepared by paint-thermal decomposition. *J. Photochem. Photobiol. A Chem.*, 305: 83-92.
- Chong, M.N., B. Jin, C.W. Chow and C. Saint, 2010. Recent developments in photocatalytic water treatment technology: A review. *Water Res.*, 44: 2997-3027.
- Cotal, H., C. Fetzer, J. Boisvert, G. Kinsey and R. King *et al.*, 2009. III-V multijunction solar cells for concentrating photovoltaics. *Energy Environ. Sci.*, 2: 174-192.
- Daskalaki, V.M., I. Fulgione, Z. Frontistis, L. Rizzo and D. Mantzavinos, 2013. Solar light-induced photoelectrocatalytic degradation of bisphenol-A on TiO<sub>2</sub>/ITO film anode and BDD cathode. *Cata. Today*, 209: 74-78.
- Demeestere, K., J. Dewulf and H.V. Langenhove, 2007. Heterogeneous photocatalysis as an advanced oxidation process for the abatement of chlorinated, monocyclic aromatic and sulfurous volatile organic compounds in air: State of the art. *J. Environ. Sci. Technol.*, 37: 489-538.
- Detle, C., M.A. Perez-Osorio, C.S. Kley, P. Punke and C.E. Patrick *et al.*, 2014. TiO<sub>2</sub> anatase with a bandgap in the visible region. *Nano Lett.*, 14: 6533-6538.
- Fan, L., Y. Zhou, W. Yang, G. Chen and F. Yang, 2006. Electrochemical degradation of amaranth aqueous solution on ACF. *J. Hazard. Mater.*, 137:1182-1188.
- Han, L., F.F. Abdi, R.V.D. Krol, R. Liu and Z. Huang *et al.*, 2014. Efficient water-splitting device based on a bismuth vanadate photoanode and thin film silicon solar cells. *Energy Mater. Sustainability*, 7: 2832-2838.
- Huang, J., Y. Shao and Q. Dong, 2015. Organometal trihalide perovskite single Crystals: A next wave of materials for 25% efficiency Photovoltaics and applications beyond?. *J. Phys. Chem. Lett.*, 6: 3218-3227.
- Martinez-Huitle, C.A. and E. Brillas, 2009. Decontamination of wastewaters containing synthetic organic dyes by electrochemical methods: A general review. *Applied Catal. B-Environ.*, 87: 105-145.
- Sarkka, H., A. Bhatnagar and M. Sillanpaa, 2015. Recent developments of electro-oxidation in water treatment-a review. *J. Electr. Chem.*, 754: 46-56.
- Tyagi, V.V., N.A. Rahim, A. Jeyraj and L. Selvaraj, 2013. Progress in solar PV technology: Research and achievement. *Renewable Sustainable Energy Rev.*, 20: 443-461.